The Effects of Inlet Flow Modification on Cavitating Inducer Performance

J. Del Valle

D. M. Braisted

C. E. Brennen

California Institute of Technology, Pasadena, CA 91125

This paper explores the effect of inlet flow modification on the cavitating and noncavitating performance of two cavitating inducers, one of simple helical design and the other a model of the low-pressure LOX pump in the Space Shuttle Main Engine. The modifications were generated by sections of honeycomb, both uniform and nonuniform. Significant improvement in the performance over a wide range of flow coefficients resulted from the use of either honeycomb section. Measurements of the axial and swirl velocity profiles of the flows entering the inducers were made in order to try to understand the nature of the inlet flow and the manner in which it is modified by the honeycomb sections.

1 Introduction

The purpose of this report is to document one effort to determine the effect of inlet flow modification on the performance of pumps, in particular axial flow inducers under cavitating and noncavitating conditions. Many test facilities, including that used for the present tests, take care to ensure a quite uniform velocity profile in the flow at inlet to the pump being tested. Yet frequently the prototype must function with inlet flows that are quite distorted and nonuniform. For example, aircraft fuel pumps frequently have a 90 deg bend just upstream of the leading edge of the impeller (Grennan, 1978). Moreover, manufacturers of axial flow pumps are often not free to provide a sufficient length of inlet ducting to ensure that the performance is unaffected by whatever inlet piping the customer chooses to attach to the pump.

The focus of the present paper will be on those inlet flow distortions produced by asymmetries in the structure. However, it should also be recognized that, particularly at flow rates below design, nonuniform axial velocities and swirl velocities may be generated by backflow from the impeller itself and the associated prerotation (Acosta, 1958; Toyokura, 1961; Badowski, 1970; Janigro and Ferrini, 1973). We delay further discussion of this until section 5.

Inlet flow distortion will have a number of consequences. Even in the absence of cavitation, nonuniform axial velocities or swirl velocities could lead to deviations from the design angles of attack and therefore to alteration in performance. If the pump is cavitating, the circumferential variation in the effective cavitation number could lead to cavities that, on a particular blade, grow and collapse during one rotation of the impeller in much the same way as cavities grow and collapse on the blade of a ship's propellor due to changes in hydrostatic pressure during a revolution. This would lead to deterioration in the cavitation performance and increase in the levels of noise and cavitation damage. Although the results that emerged were somewhat different, one of the initial objectives of this study was to examine some of these effects on the steady-state hydraulic performance of typical axial flow inducers.

There are, however, other potential effects of inlet flow distortion that, though not addressed in this report, nevertheless deserve mention. In modern high-speed pumps one is concerned with the radial loads and rotordynamic forces imposed on the impeller by the flow. Large radial loads on the impeller can cause excessive bearing wear or failure and large rotordynamic forces can lead to large or unstable whirl motions (Brennen et al., 1986; Jery et al., 1985). It is probable that inlet flow distortion could produce substantial lateral loading. In addition to overall impeller loads, one must also be concerned with the dynamic loading on individual impeller blades. Recently, Arndt et al. (1989) have shown that the unsteady loads on diffuser blades due to the passage of an upstream impeller blade can be much larger than the time-averaged load. While this is a function of the gap between the rotor and stator blades, Arndt et al. measured unsteady loads with amplitudes as large as three times the time-averaged load. In the present context this leads one to be concerned about the loads on individual inducer blades caused by wakes or other flow distortion in the inlet flow. A current project in our laboratory is directed toward measuring some of these loads and these concerns will therefore be addressed at a later date.

Another concern might be the extent to which inlet flow distortion might affect the dynamic rather than static hydraulic performance of the pump. This would result in changes in the limits of stable operation of the pump. Braisted (1979) showed that installation of flow-straightening devices in the inlet could cause changes in both the onset and frequency of auto-oscillation of cavitating inducers. However, some measurements of the dynamic transfer functions for those same inducers (in the manner described by Brennen et al., 1982) with and without

Contributed by the International Gas Turbine Institute for publication in the JOURNAL OF TURBOMACHINERY. Manuscript received by the International Gas Turbine Institute September 1991. Associate Editor: L. S. Langston.

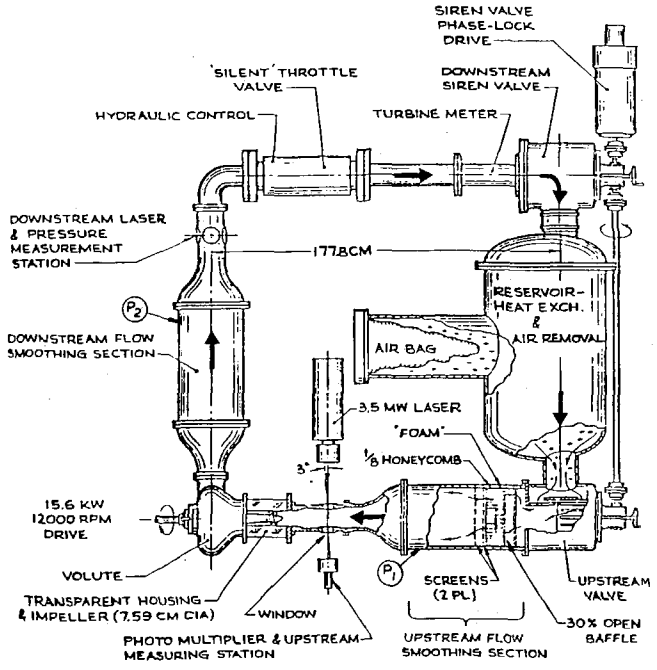

Fig. 1 Schematic of the Dynamic Pump Test Facility (DPTF)

the flow straighteners indicated very little measurable effect of the flow straighteners on those transfer functions.

2 Dynamic Pump Test Facility and Test Impellers

The facility used for the measurement of the effects of both the uniform and nonuniform inlet flow straighteners on the steady-state performance of axial flow pumps and inducers is known as the Dynamic Pump Test Facility (DPTF) and is shown diagramatically in Fig. 1. This system was originally designed to measure not only the steady-state characteristics of cavitating inducers but also transfer functions and other dynamic characteristics under cavitating and noncavitating conditions; further details can be found from Ng (1976) and Ng and Brennen (1978). It will be suffice here to discuss only those aspects pertinent to the measurement of the steady-state performance of the impellers.

The mean flow rate at a particular rotational pump speed was adjusted by means of a hydraulically operated throttle valve, labeled the "silent" throttle valve in Fig. 1. Just downstream of this is a turbine flow meter, which was used for both measurement of the mean flow rate and also as a signal input to a hydraulic servo system, which operated the "silent" valve and thereby maintained a preset value of the mean flow in the pump loop.

The pressure level in the circuit was controlled by means of air pressure regulation of the interior of a large plastic bag that communicates with the large tank, as shown in Fig. 1. This reservoir was also used to maintain constant temperature by means of a heat exchanger and for the collection and removal of air from the circuit.

The primary mean pressure measurements were made using pressure transducers placed near the downstream end of the two smoothing chambers as shown by P_1 and P_2 in Fig. 1. These were calibrated prior to each experiment against an accurate Heise gage. The calibrations were both linear and repeatable. The steady or mean pressure rise across the pump was determined from the difference in the two pressure transducer measurements. The total pressure drop across the elements of the downstream smoothing section was measured and found to be negligible in comparison.

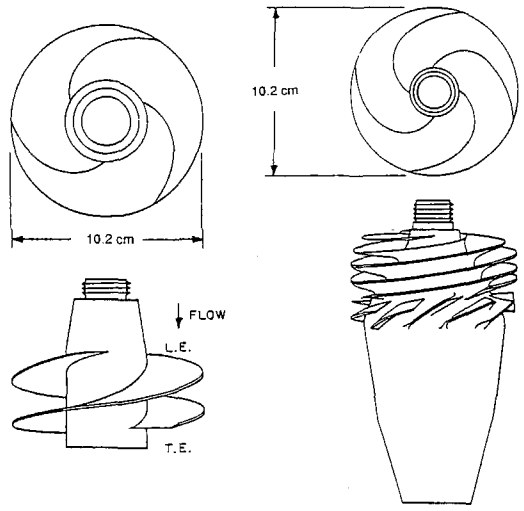

Fig. 2 Inducers used in present experiments: Impeller VII (left) is a 9 deg helical inducer; Impeller VI (right) is a model of the low-pressure LOX impeller in the Space Shuttle Main Engine

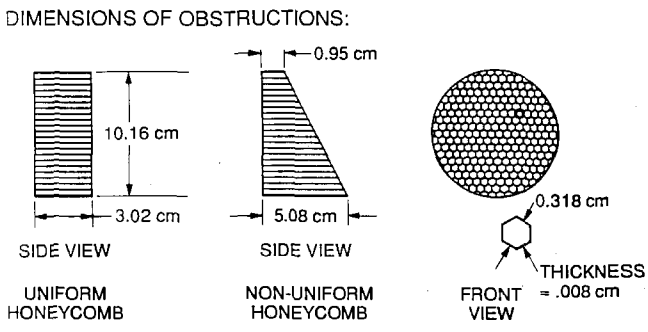

Fig. 3 Schematic showing the shape and positioning of both the uniform and nonuniform honeycomb devices installed in the impeller inlet flow

Two different impellers were used in the present experiments and these are sketched in Fig. 2. One, designated Impeller VII, was a simple 9 deg helical inducer (10.2 cm in diameter) with swept leading edges and made from stainless steel. The other, Impeller VI, was an accurate aluminum model (about 1/3 scale) of the low-pressure oxidizer turbopump in the Space Shuttle main engine. More detailed information on these impellers is contained in the works by Ng (1976) and Ng and Brennen (1978).

3 Modifications of the Inlet Flow

The purpose of the present tests was to investigate the dependence of the pump performance on inlet flow distortion. It was therefore, necessary to design devices that would impose simple and calibrated distortions on the inlet flow. Develop-

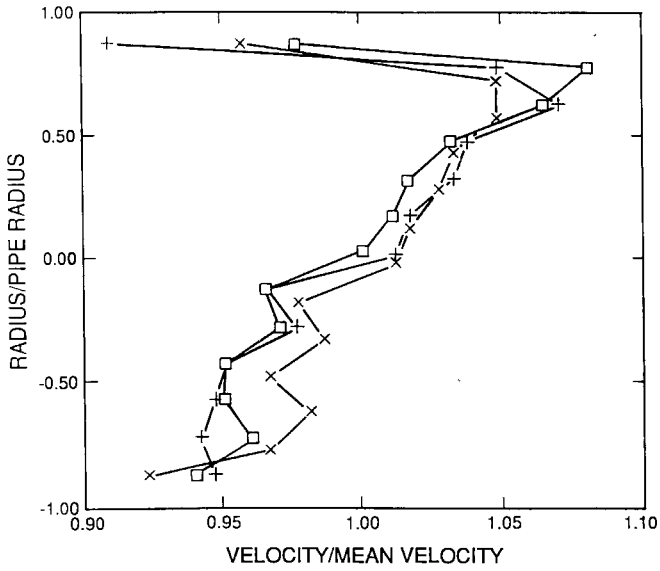

Fig. 4 Velocity profiles (measured in air tunnel) 9.52 cm downstream of the nonuniform honeycomb as a function of radial position within the 10.2-cm-dia pipe. Data for mean velocity of 9.4 m/s: × ; for 8.78 m/s: □ , for honeycomb rotated one half-turn and velocity of 9.4 m/s: + .

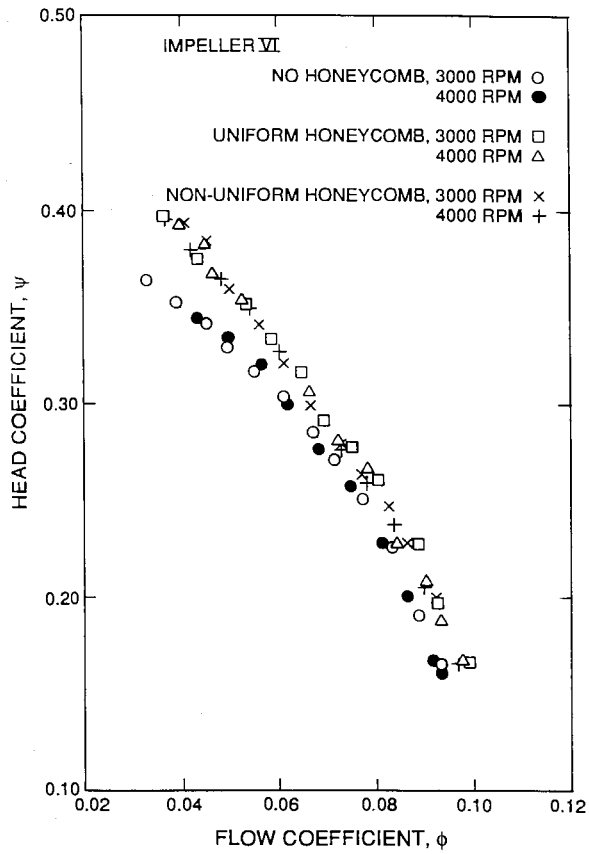

Fig. 5 Dimensionless, noncavitating performance of impeller VI at various speeds and with and without the honeycomb devices installed in the inlet flow

ment of such devices was most readily done in a small air tunnel using velocities that corresponded to the appropriate Reynolds scaling. Since the typical inlet axial velocity of water in the DPTF was about 1.8m/s, the air tunnel (whose working section was a piece of 10.2-cm-dia pipe) was operated at a mean velocity of about 10m/s.

Many different obstructions made from metal honeycomb with very thin walls (0.008 cm thick) were tested in this air

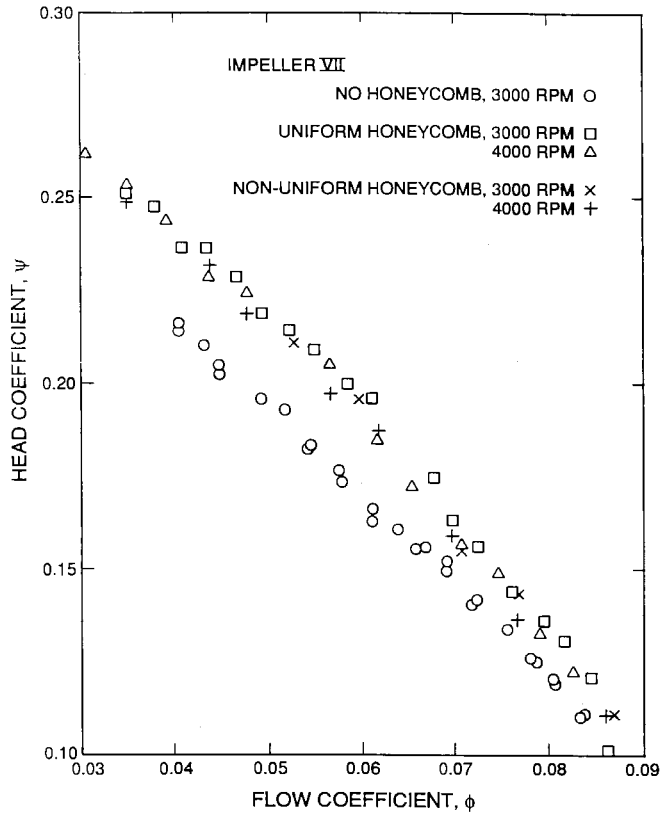

Fig. 6 Dimensionless, noncavitating performance of impeller VII at various speeds and with and without the honeycomb devices installed in the inlet flow

tunnel. Measurements of the velocity profiles resulting from these obstructions were made with a hot-wire anemometer at a distance 9.52 cm downstream of the trailing edge of the obstruction. It was concluded that the tapered or nonuniform honeycomb insert shown in Fig. 3 produced an appropriate nonuniformity consisting of a relatively simple shear flow.

Three different velocity distributions resulting from this nonuniform honeycomb measured in the air tunnel are shown in Fig. 4. Two of these are at mean velocities that differ by about 10 percent. The other was taken with the obstruction rotated by 180 deg in order to distinguish between nonuniformities produced by the honeycomb and any that might have been inadvertently introduced by the facility. The profiles are all essentially the same and represent a flow with a shear of about 10 percent between the extremes of a diameter. The fact that the profile is unchanged by rotation of the orientation of the honeycomb provides assurance that the nonuniformity is due to the honeycomb.

Because initial results from the steady-state performance tests using the obstruction differed significantly from those without one, it was decided that a second "uniform" obstruction should be included in the testing so as to deduce how much of the effect was attributable to factors other than the nonuniformity of the profile such as, for example, the flow straightening effect of the honeycomb. Both obstructions and their location relative to the impeller are shown in Fig. 3.

4 Steady-State, Noncavitating Performance

In order to determine the effects of the inlet flow obstructions on the steady-state performances of both impellers, a variety of experiments were conducted. The first series of tests involved measurements of the steady-state, noncavitating hydraulic performance of the two impellers at speeds of both 3000 and 4000 rpm. The flow rate was measured using cali-

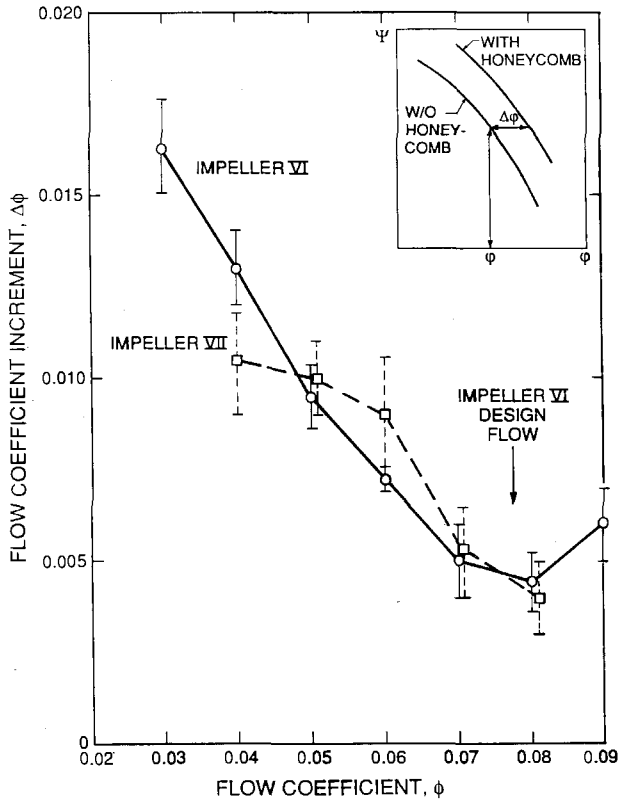

Fig. 7 The flow coefficient increment, $\Delta\varphi$, caused by the honeycomb inserts as a function of the flow coefficient, φ, in the absence of the inserts

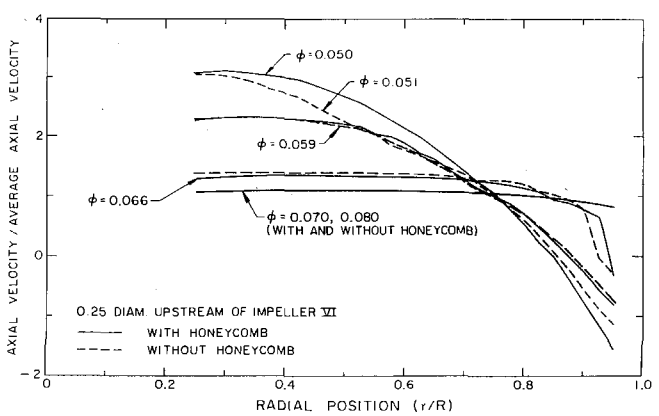

Fig. 8 Axial velocity profiles 0.25 diameters upstream of Impeller VI at various flow coefficients, φ, and with (———) and without (– – –) honeycomb inserts. Data points taken each $\Delta(r/R) = 0.025$ have been omitted for clarity; uncertainty is ± 0.05 on the ordinate.

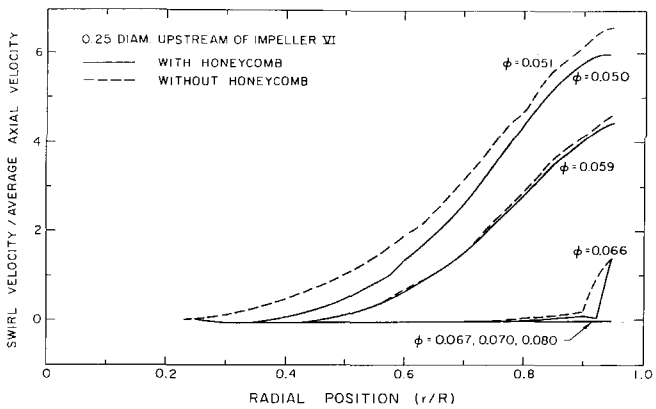

Fig. 9 Swirl velocities corresponding to the axial velocities of Fig. 8

brated turbine flow meter (Fig. 1) and the total head was measured in the upstream and downstream smoothing sections shown in Fig. 1. Note that the inlet total head is therefore measured upstream of the honeycomb inserts. Data were taken at two speeds in order to check for any significant Reynolds number effects. As will be seen in Figs. 5 and 6, no such effect was discernible and hence the data for the two speeds will be treated as one larger set. The hydraulic performance under noncavitating conditions is presented as follows. The total head rise, ΔH, is converted to a head coefficient, ψ, by dividing by ρu_T^2 (where ρ is fluid density and u_T is the inducer tip speed) and plotted against the flow coefficient, φ, obtained by nondimensionalizing the flow rate by Au_T where A is the inlet area, πr_T^2, where r_T is the inducer tip radius. Data for both impellers with no honeycomb, with the uniform honeycomb and with the nonuniform honeycomb, are presented in Figs. 5 and 6.

Several conclusions can be drawn from these data. First the installation of either of the honeycombs has caused a substantial increase in the pump performance. Later we examine the possibility that this effect may be the result of the attenuation of the induced prerotation or inlet swirl caused by any honeycomb. By fitting curves to the data with and without a honeycomb insert, we plot in Fig. 7 the incremental increase in flow caused by the insertion of the honeycomb as a function of the flow coefficient without the honeycomb. Both impellers yield very similar results, the improvement being larger at flow coefficients below the design values. The incremental flow coefficients imply changes in the angle of attack at the inducer tip of less than a degree (0.29 deg at $\Delta\varphi = 0.005$ to 0.86 deg at $\Delta\varphi = 0.015$).

The second major conclusion to be drawn from Figs. 5 and 6 is that one cannot discern any effect of the nonuniform honeycomb relative to the uniform honeycomb. The effect that either honeycomb has in inhibiting prerotation is much larger than the effect of the nonuniformity introduced by the nonuniform honeycomb. Indeed, any artifact that could introduce nonuniformity would also affect prerotation and one conclusion that can be drawn from these tests is that the change in prerotation may dominate any effect of nonuniformity, at least insofar as hydraulic performance is concerned.

5 Swirl and Axial Velocity Profiles

To investigate these effects in more detail, inlet axial and swirl velocity profiles were obtained by means of a wedge probe and total head traverses (Braisted, 1979). The wedge probe was used to determine the direction of the flow and subsequent total head probe measurements were made using these angles. Profiles for the swirl and axial velocities were calculated from these measurements by assuming radial equilibrium, which previous investigations have established as valid for these inlet flows (Janigro and Ferrini, 1973). Data taken 0.25 diameters upstream of the leading edge of Impeller VI are shown in Figs. 8 and 9; similar data 0.5 diameters upstream are included in Figs. 10 and 11. Data were taken at both 4000 and 6000 rpm but yielded essentially the same profiles at the two speeds.

These velocity profiles are consistent with those measured previously (Badowski, 1970). They clearly show that the annular jet produced by the tip clearance flow occurs below a certain critical flow coefficient (φ_c) and penetrates farther upstream the lower the flow coefficient (see also Acosta, 1958). The variation of the critical flow coefficient with Reynolds number and hub-to-tip ratio has recently been explored by Alpan and Peng (1989). In Figs. 8, 9, 10, and 11 the backflow

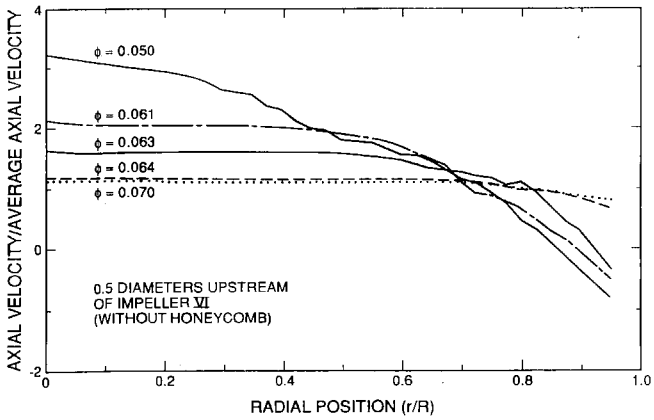

Fig. 10 As Fig. 9 but 0.5 diameters upstream of Impeller VI

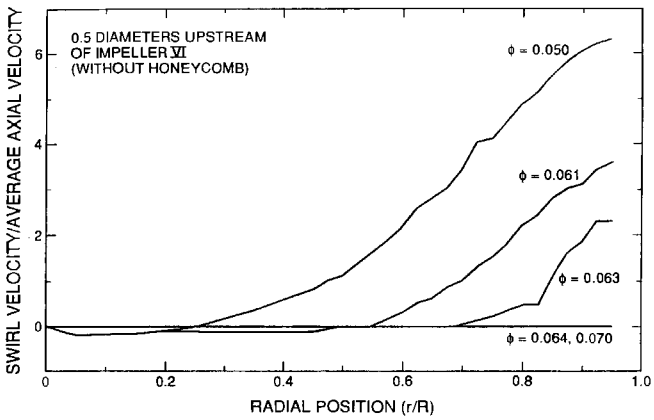

Fig. 11 Swirl velocities corresponding to the axial velocities of Fig. 10

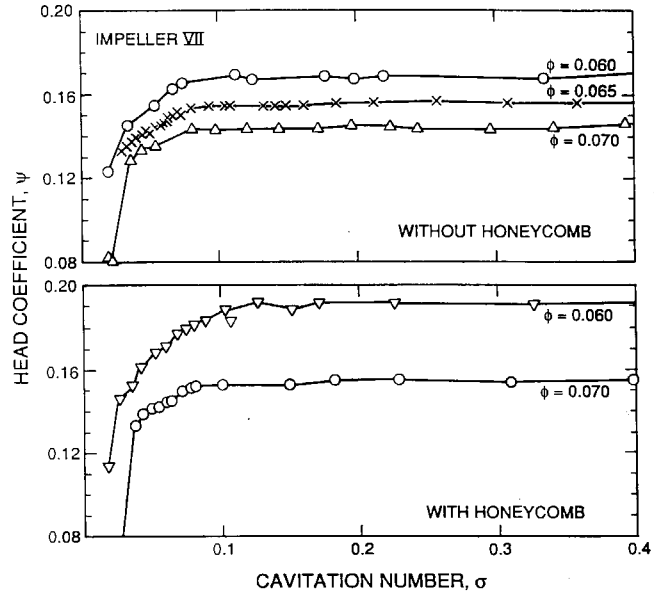

Fig. 12 Cavitation performance for Impeller VII at 7000 rpm and various flow coefficients, φ, as indicated and with and without honeycomb insert

can be clearly identified as the region of negative axial velocity. Note from Figs. 8 and 10 that the backflow has penetrated 0.25 diameters upstream at $\phi \approx 0.067$ and 0.5 diameters upstream at $\varphi \approx 0.064$. As discussed by Badowski (1970) and Murakami and Heya (1966), the backflow is the source of the vorticity or swirl velocity. At higher flow coefficients above the critical the backflow vanishes and the swirl is essentially zero as it must be from Kelvin's theorem. However, we can also see that, in the presence of backflow, the nonzero swirl velocities are not confined to the backflow region. Braisted (1979) has observed that this inward diffusion of vorticity occurs much too rapidly to be caused by molecular viscosity. Thus it would appear that the high degree of turbulence and unsteadiness in this flow must cause the diffusion of swirl over almost the entire cross section of the inlet flow.

The data of Fig. 9 indicate that, as earlier surmised, the honeycomb insert reduces the prerotation or swirl, at least at low flow coefficients. However this does not explain the favorable effect of the honeycomb over the entire range of flow coefficients; even at the lower flow coefficients the changes in prerotation exhibited in Fig. 9 seem too small to explain the change in performance. We conclude that, as yet, there is no satisfactory explanation for the performance enhancement caused by the honeycomb. These inlet flows are very unsteady and one might speculate that this unsteadiness may well affect performance adversely. If the honeycomb dampens this unsteadiness, then that might provide a possible explanation for the observed effects.

One tenuous previously mentioned piece of evidence that might support such an explanation emerges from the work of Braisted (1979) on the auto-oscillation of the same cavitating inducers. Braisted observed that both the onset and frequency of auto-oscillation were affected by the presence of the honeycomb in the inlet flow. For example, the frequency of auto-oscillation of Impeller VII was increased by about 20 percent by the insertion of the honeycomb. This suggests a significant change in dynamics of the flow.

6 Cavitation Performance

Cavitation performance measurements were made with both impellers at several speeds and flow coefficients and with and without honeycomb inserts. More details on the procedures used for these tests may be found in Ng (1976) and Braisted (1979). For example, the tests were all performed after substantial de-aeration of the water in the facility. Typical nondimensional results are presented in Fig. 12 and 13 where the head coefficient, ψ, for a given flow coefficient, ϕ, is plotted against the cavitation number defined as $\sigma = (p_1 - p_v)/1/2\rho u_T^2$ where p_1 and p_v are respectively the inlet static pressure and the vapor pressure at the operational water temperature. The data exhibit the conventional breakdown characteristics, which were more readily documented for the helical Impeller VII than for the more advanced and better-performing Impeller VI because the former begins to break down at higher cavitation numbers.

The first conclusion to be drawn from these tests represents an extension of the earlier conclusion on the effect in noncavitating flow, namely that the results for the uniform and nonuniform honeycomb were essentially identical but differed from the performance without any honeycomb. Consequently we compare in Figs. 12 and 13 the cavitation performance with and without a honeycomb. When the data of Fig. 12 are compared one can see that the cavitation performance at $\varphi = 0.070$ with the honeycomb is essentially the same as the data at $\varphi = 0.065$ without the honeycomb and that the rest of the data are also consistent with a similar shift in the effective flow coefficient of the order of 0.005. Hence we may expand the other principal conclusion that emerged from the noncavitating performance data, namely, that the cavitation performance change caused by the honeycomb inserts can be described simply as an effective change in the flow coefficient as given in Fig. 7.

Parenthetically we note that Braisted (1979) found that some inlet velocity profile measurements under cavitating conditions ($\sigma = 0.1$) indicated that the profiles are not greatly effected by

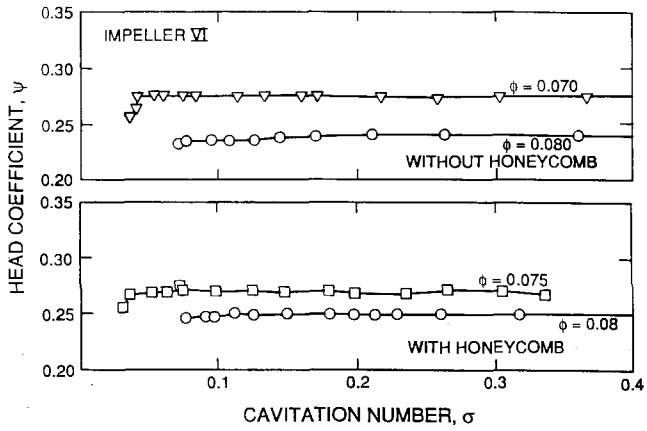

Fig. 13 Cavitation performance for Impeller VI at 6000 rpm and various coefficients, φ, as indicated and with and without honeycomb insert

the presence of cavitation as long as one is above the value of σ at which the head is significantly affected.

7 Conclusions

Sections of honeycomb installed in the inlet flow to two cavitating inducers caused a substantial improvement in the hydraulic performance of those inducers. This performance enhancement, which could be characterized by an increase in the flow coefficient, $\Delta\varphi$, at the same head rise, occurred over a wide range of flows, though it was greater below the design flow coefficient. The changes in both the noncavitating and cavitating performance could be represented by a change in the effective flow coefficient designated the flow coefficient increment, $\Delta\varphi$. The increment and its dependence on the flow coefficient were similar for the two inducers tested. Parenthetically we should note that the improvement referred to above applies to an increase in the head rise for a given flow. The effect on efficiency was not measured and would be interesting to investigate.

Honeycomb sections that were both uniform and nonuniform were tested, the latter in an attempt to evaluate the effect of nonuniform axial velocity profiles on inducer performance. However, if such an effect exists, it was much smaller than the change occurring with and without honeycomb inserts.

Measurement of axial and swirl velocity profiles were made in order to provide further documentation of the actual inlet flow at two locations, 1/4 and 1/2 diameter upstream of the inlet plane of one of the inducers. These measurements are consistent with the previous measurements of Badowski (1970) and confirm that, as the loading is increased (φ decreased), the backflow jet generated by the tip clearance flow is initiated at a certain critical flow coefficient, φ_c, and penetrates farther upstream with further decrease in φ. Nonzero swirl velocities (prerotation) only occur for $\varphi < \varphi_c$. However, the swirl is not confined to the backflow jet; the vorticity from this jet is diffused inward so that swirl velocities are measured over virtually all of the inflow. The mechanism for such rapid diffusion of vorticity must be turbulent convection resulting from the high degree of unsteadiness associated with the backflow.

Velocity profiles were obtained with and without the honeycomb flow straightener installed. While this device caused some decrease in the swirl velocity at inlet to the inducer, it appears insufficient to explain the performance enhancement which the device caused over the full range of flow coefficient.

Acknowledgments

The authors would like to thank NASA George Marshall Space Flight Center for support of this research under Contracts NAS8-29313, NAS8-29046, and Grant No. NAG8-118.

References

Acosta, A. J., 1958, "An Experimental Study of Cavitating Inducers," *Proc. Second Symp. on Naval Hydrodynamics*, ONR/ACR-38, pp. 533–557.

Alpan, K., and Peng, W. W., 1989, "Suction Reverse Flow in an Axial-Flow Pump," *ASME Symp. on Pumping Machinery—1989*, ASME FED-Vol. 81, pp. 141–148.

Arndt, N., Acosta, A. J., Brennen, C. E., and Caughey, T. K., 1989, "Rotor-Stator Interaction in a Diffuser Pump," ASME JOURNAL OF TURBOMACHINERY, Vol. 111, pp. 213–221.

Badowski, H. R., 1970, "Inducers for Centrifugal Pumps," Internal report, Worthington Canada, Ltd.

Braisted, D. M., 1979, "Cavitation Induced Instabilities Associated With Turbomachines," Ph.D. thesis and Eng. and Appl. Sci. Report No. E184.2, California Institute of Technology, Pasadena, CA.

Brennen, C. E., and Braisted, D. M., 1980, "Stability of Hydraulic Systems With Focus on Cavitating Pumps," *Proc. 10th Symposium of IAHR*, Tokyo, Japan.

Brennen, C. E., Meissner, C., Lo, E. Y., and Hoffman, G. S., 1982, "Scale Effects in the Dynamic Transfer Functions for Cavitating Inducers," ASME *Journal of Fluids Engineering*, Vol. 104, pp. 428–433.

Brennen, C. E., Acosta, A. J., and Caughey, T. K., 1986, "Impeller Fluid Forces," *NASA Prod. Advanced Earth-to-Orbit Propulsion Technology Conference*, Huntsville, AL, NASA Conf. Publ. 2436, pp. 270–295.

Grennan, C. W., 1978, "Polyphase Flow in Gas Turbine Fuel Pumps," in: *Polyphase Flow in Turbomachinery*, C. Brennen, P. Cooper, and P. W. Runstadler, eds., ASME, New York.

Janigro, A., and Ferrini, F., 1973, "Inducer Pumps," in: *Recent Progress in Pump Research*, von Karman Inst. for Fluid Dynamics, Lecture Series 61.

Jery, B., Acosta, A. J., Brennen, C. E., and Caughey, T. K., 1985, "Forces on Centrifugal Pump Impellers," presented at the Second International Pump Symposium, Houston, TX, Apr. 29–May 2, 1985.

Murakami, M., and Heya, M., 1966, "Swirling Flow in Suction Pipe of Centrifugal Pumps," *Bull. Japanese Soc. Mech. Eng.*, Vol. 9, No. 34.

Ng, S. L., 1976, "Dynamic Response of Cavitating Turbomachines," Ph.D. Thesis and Eng. and Appl. Sci. Report No. E183.1, California Institute of Technology, Pasadena, CA.

Ng, S. L., and Brennen, C., 1978, "Experiments on the Dynamic Behavior of Cavitating Pumps," ASME *Journal of Fluids Engineering*, Vol. 100, No. 2, pp. 166–176.

Toyokura, T., 1961, "Studies on the Characteristics of Axial-Flow Pumps," Parts 1–6, *Bull. Japan. Soc. Mech. Eng.*, Vol. 4, pp. 287–340.